ANALYTICAL SOLUTIONS FOR WALL SLIP EFFECTS ON MAGNETOHYDRODYNAMIC OSCILLATORY ROTATING PLATE AND CHANNEL FLOWS IN POROUS MEDIA USING A FRACTIONAL BURGERS VISCOELASTIC MODEL

Khadija Maqbool[1], O. Anwar Bég[2], Ayesha Sohail[3] and Shafaq Idreesa[3]*
[1] Department of Mathematics & Statistics, FBAS, IIUI, Islamabad 44000, Pakistan.
[2]Fluid Mechanics, Spray Research Group, Mechanical and Petroleum Engineering, School of Computing, Science and Engineering, G77, Newton Building, University of Salford, Manchester, M54WT, UK.
[3] Department of Mathematics, Comsats Institute of Information Technology, Lahore 54000, Pakistan

*Corresponding author- Email: O.A.Beg@salford.ac.uk

ABSTRACT
A theoretical analysis of magnetohydrodynamic (MHD) incompressible flows of Burger's fluid through a porous medium in a rotating frame of reference is presented. The constitutive model of a Burger's fluid is used based on a fractional calculus formulation. Hydrodynamic slip at the wall (plate) is incorporated and a fractional generalized Darcy model deployed to simulate porous medium drag force effects. Three different cases are considered- namely, flow induced by a general periodic oscillation at a rigid plate, periodic flow in a parallel plate channel and finally Poiseuille flow. In all cases the plate (s) boundary (ies) are electrically-non-conducting and small magnetic Reynolds is assumed, negating magnetic induction effects. The well-posed boundary value problems associated with each case are solved via Fourier transforms. Comparisons are made between the results derived with and without slip conditions. 4 special cases are retrieved from the general fractional Burgers model, viz *Newtonian fluid, general Maxwell viscoelastic fluid, generalized Oldroyd-B fluid and the conventional Burger's viscoelastic model*. Extensive interpretation of graphical plots is included. We study explicitly the influence on wall slip on primary and secondary velocity evolution. The model is relevant to MHD rotating energy generators employing rheological working fluids.

Key words: *Magnetohydrodynamics (MHD); Non-Newtonian; Fractional Burger fluid; Oscillation; Slip; Porous medium; Fourier transforms; MHD energy generators*.

1. INTRODUCTION

Significant attention has been given to physico-mathematical and computational simulations in non-Newtonian fluid physics in recent years. These stem from ever-widening applications of such fluids in medical engineering (gels, drugs, creams etc) [1], plastics fabrication [2], industrial adhesives and lubricants [3] and also environmental systems including hyper-concentrated sediments, oil spills, mud flows and contaminant release [4]. The intrinsic properties of non-Newtonian or rheological fluids invalidate the conventional Navier-Stokes viscous model

(Newtonian). Phenomena such as shear-thinning/thickening, yield stress, fading memory, re-coil, micro-structure, relaxation, retardation, elongation, stress differences, spurt, Weissenberg effects and many others simply are not reproducible within the framework of Newtonian fluid dynamics. An excellent appraisal of the departure of rheological fluids from Newtonian behavior has been provided by Chaabra and Richardson [5] and also more recently by Irgens [6]. Viscoelastic fluids belong to the class of non-Newtonian fluids which exhibit both viscous and elastic effects, in varying proportions depending on the constitution of the liquid. They are a special class of non-Newtonian fluids which sustain normal stress difference in flow fields. A seminal discussion of many aspects of viscoelastic hydrodynamics has been given in the monograph of Joseph [7]. Viscoelastic fluids have been analyzed with many different constitutive formulations, including the Maxwell fluid model [8], Oldroyd-B fluid model [9], Reiner-Rivlin differential second and third grade fluid models [10, 11], Jefferys model [12], Sisko's model [13], Walters-B model [14] and Burger's elasto-viscous fluid model [15] are typical viscoelastic models and have been implemented in numerous studies in chemical, environmental and also medical engineering systems. Certain models of viscoelastic fluids are based on the so-called fractional derivatives which employs Leibnitz theory of differentiation to arbitrary non-integers (fractions). Early applications of fractional calculus in rheology include the work of Scott Blair *et al*. [16] and Graham *et al.* [17]. Fractional models essentially replace the ordinary time derivatives by fractional order time derivatives, and this plays an important role in more realistically simulating real viscoelastic properties of these liquids. This is usually achieved by employing Riemann-Louville fractional calculus operators although other approaches do exist. Many analyses of viscoelastic fluids employing fractional derivatives have been communicated in recent years. Representative studies in this regard include Lei *et al*. [18] who derived both local and global smooth solutions to the Cauchy problem in the whole space and the periodic problem in the *n*-dimensional torus for incompressible viscoelastic fractional Oldroyd-B fluids, also demonstrating the validity of this approach to elastic complex fluids, magnetic rheological fluids, liquid crystal and mixture suspensions. Lin *et al.* [19] determined both local and global existence of classical solutions for a fractional Oldroyd fluid in the absence of an artificially postulated damping mechanism. Wang and Xu [20] investigated transient axial Couette flows of both fractional second grade fluid (FSGF) and fractional Maxwell fluid (FMF) between two infinitely long concentric circular cylinders, observing that via an analysis of fractional derivative on the models via numerical results,

oscillations exist in the FMF velocity field. Tong and Liu [21] investigated analytically the unsteady rotational flows of an Oldroyd-B fluid in an annular pipe, constructing also a generalized Jeffreys model via fractional calculus. They showed that the classical Navier–Stokes and also Maxwell fluid and second grade fluid solutions may be extracted as special cases of the fractional viscoelastic model. Khan *et al*. [22] have derived exact solutions for transient starting flow of fractional Burger's fluid in the gap between two infinitely long concentric circular cylinders, both for the case where the outer cylinder makes a simple harmonic oscillation and also when the outer cylinder suddenly begins rotating while the inner cylinder remains stationary. Further appraisals of fractional viscoelastic flows have been made by Bagley and Torvik [23], Song and Jiang [24], Hilfer [25], Qi and Xu [26] and also Qi and Jin [27].

The above studies have generally assumed the *classical no-slip boundary condition* at the surface of the body in contact with viscoelastic shearing flow. This condition, which is characteristic of Navier-Stokes formulations, is in fact quite unrealistic for non-Newtonian flows. Hydrodynamic slip is a very sophisticated phenomenon which involves the non-adherence of fluids to surfaces. It can manifest physically in polymers as a result of the formation of a resin rich, low viscosity layer adjacent to the wall or loss of adhesion with the wall. Slip in other complex rheological suspensions can be generated via dismantling of network structures in the region near the wall and the development of a thin lubricating layer generated by flow-induced diffusion. Slip is also intimately associated with wall surface texture and material rheology of fluids and is a common feature in colloidal crystal material dynamic as well as plastic extrusion systems and magnetohydrodynamic generator flows. Here we are concerned with wall slip (rather than interfacial particle-particle slip) and this type of boundary slip can be delineated into `true slip' where there is a discontinuity in the velocity field at the fluid-solid interface, and `apparent slip' where there is an inhomogeneous thin layer of fluid adjacent to the wall with different rheological properties to the bulk of fluid which facilitates fluid movement. Causes for the latter may be large velocity gradients across the very thin low-viscosity slip layer which mimick slip at the wall although generally the no-slip condition is not violated. Both true and apparent slip have been verified experimentally and the general consensus is that apparent slip actually is the more typical mechanism for observed wall slip in polymers and the so-called true slip is in fact not responsible for tangible macroscopic slip. Molecular forces between the fluid and solid are known to impede the motion of non-Newtonian fluid at the wall-fluid interface. In any event, wall slip cannot and should not be neglected in

realistic polymer rheological flows as it has significant effects on manufactured products. Serious investigations of slip in polymer dynamics were initiated many decades ago by Mooney [28] at the United States Rubber Corporation, who developed simple formulations for quantifying slip based on a hydrodynamical theory of a Newtonian fluid flowing through a capillary viscometer. More recent efforts have addressed slip effects in non-Newtonian flows. Betola [29] investigated wall slip effects on viscoelastic foam drainage, identifying that while fluid elasticity exerts no tangible influence on drainage velocity, with wall slip incorporated a faster drainage velocity is achieved. Mohseni and Rashidi [30] studied theoretically the axial annular flow of Giesekus viscoelastic fluid with dual wall slip effects, observing that slip is initiated first at the inner wall and thereafter at the outer wall and identifying three flow regimes, namely the no slip condition, slip only at the inner wall and slip at both walls. They further noted that with greater elastic effects, slip is reduced at the wall and that increasing slip effect depresses pressure gradient, shear and normal stresses whereas an increase in slip critical shear stress induces the opposite effect. Further studies of viscoelastic slip flows include Abelman *et al*. [31] who employed a third grade Reiner-Rivlin differential model to examine rotating Couette flows and Tripathi *et al.* [32] who used a fractional Oldroyd-B model to simulate peristaltic propulsion with wall slip. In recent years a new generation of fluids termed magneto-active polymers has emerged [33]. These intriguing materials exhibit both viscoelastic and magnetic properties. They include ferrogels [34] which comprises a gel-like matrix and magnetic particles which are randomly distribute in the matrix. The gel bulk matrix viscoelasticity leads to rate-dependent behaviors. Magnetic characteristics include ferrohydrodynamic (FHD) and magnetohydrodynamic (MHD) behavior i.e. such materials response to applied magnetic fields (owing to their electro-conductive nature). In the synthesis of such materials, slip flows also arise as with conventional polymeric fluids. This has motivated many researchers to investigate magneto-viscoelastic fluid dynamics which has potential relevance to both materials processing and also to working fluids in novel MHD energy generators. A relatively recent summary of ferrogel dynamics is documented in Bég *et al.* [35] wherein Lorentzian drag, Ohmic dissipation, magnetic induction, dipole, Hall current and other effects are reviewed in detail. Slip flows of magneto-viscoelastic fluids are equally relevant to ferrogel fabrication and also optimization of MHD power generators in for example aerospace applications [36]. Loss mechanisms in MHD generators include wall slip, shunt currents in boundary layers and also vorticity generation and suppression. Magnetohydrodynamic slip flows for viscoelastic

materials in such systems are even more complex than for Newtonian working fluids. The latter have been examined by Martin *et al*. [37] and Fang *et al*. [38]. Magneto-viscoelastic slip flow has been studied by Zheng *et al*. [39] with the fractional Oldroyd B model.

Frequently in industrial operations including materials processing, porous media are deployed as a filter to regulate transport phenomena. Most simulations of hydrodynamic or magneto-hydrodynamic flow in porous media utilize some form of the Darcy law which is valid for viscous-dominated (low Reynolds number) scenarios and assume the medium to be fully saturated. This "drag force" approach effectively analyzes the bulk influence of solid fibers in the porous material on flow characteristics e.g. pressure, volumetric flux, velocity, shear stress etc. Although extensive analysis of Newtonian transport in porous media have been conducted, rheological flows in porous media are less frequently reported on, despite enormous applications in petro-chemical, environmental, energy systems and other technologies [40]. Studies reported have used various formulations for porous media impedance effects and deployed a diverse array of analytical and computational methods to solve the resulting boundary value problems. Tripathi and Bég [41] used the homotopy perturbation method to investigate peristaltic pumping in porous media saturated with Maxwell viscoelastic fluids, as a model of gastric transport. Niu *et al.* [42] addressed hydrodynamic stability aspects in heat transfer in Oldroyd-B viscoelastic fluid saturated porous media. Bég *et al*. [43] studied mass transfer in Maxwell viscoelastic flow in a porous medium channel. Kozicki [44] used a capillary hybrid model of viscoelastic flow in porous materials, incorporating both a viscous mode and an elongational mode, deriving relationships for friction factors and respective Reynolds numbers. Bég *et al*. [45] applied the third grade viscoelastic model to simulate convective heat transfer in boundary layer flow through a permeable half-space with both Darcy and inertial porous drag effects using a finite element algorithm. Cao *et al*. [46] used an implicit operator splitting method to study viscoelastic polymer solution flow in porous media with physicochemical reaction, employing a modified permeability model and novel relative permeability model to simulate flooding in petroleum geosystems. Further studies include Tong and Shi [47]. Magnetohydrodynamic viscoelastic flows in porous media extend these studies to consider electrically-conducting polymers. Koumy *et al.* [48] have obtained closed-form solutions for magneto-peristaltic flow of Maxwell viscoelastic fluids in porous conduits with Hall cross-flow effects. Khan and Khan [49] have investigated rotating Burgers viscoelastic MHD flow in porous media with Hall currents. Bég *et al*. [50] have employed a network electro-thermal

numerical solver to study transient magneto-viscoelastic flows in porous media. Bég *et al.* [51] have further investigated pulsating magnetized Eyring-Powell viscoelastic flow and species diffusion (mass transfer) in porous media channels as a model of drug delivery and control in the circulation system.

The present work first presents a general model for *magnetohydrodynamic (MHD) flow of an electrically-conducting fractional Burger's viscoelastic fluid from a non-conducting plate in a rotating porous medium*. Next three specific cases involving different aspects of hydrodynamic slip, periodic oscillation and other effects are studied. A similar approach for mdoelling hydrodynamic slip, albeit with thermal slip also included, has been recently presented for nanofluid slip flow in porous media by Uddin *et al.* [52]. A modified Darcy law is employed to model flow through the porous medium. Three special oscillatory MHD flow cases are examined. Exact solutions for these three cases are obtained by the Fourier transform method. Furthermore the limiting cases for viscous, second grade, Maxwell and Oldroyd-B model fluids are retracted from the generalized fractional Burgers model analyzed. The study provides a useful benchmark for numerical simulations of magnetic polymers, rheological working fluids in MHD generators etc.

2. VISCOELASTIC, ELECTROMAGNETIC AND POROUS MEDIA FORMULATIONS

The governing equation for an incompressible, Burger's viscoelastic fluid, in a rotating frame of reference may be stated as follows:

$$\rho\left(\frac{d\mathbf{V}}{dt} + (2\Omega \times \mathbf{V}) + \Omega \times (\Omega \times \mathbf{r})\right) = -\nabla\rho + div\mathbf{T} + \mathbf{J} \times \mathbf{B} + \mathbf{R}, \tag{1}$$

$$div\mathbf{V} = 0, \qquad \mathbf{V} = (u(z,t), v(z,t), 0), \tag{2}$$

where $\mathbf{T} = -p\mathbf{I} + \mathbf{S}$, denotes the Cauchy stress tensor. In eqns. (1-2), ρ is the density of fluid, p is the pressure, Ω is the angular velocity in a rotating frame, $r^2 = x^2 + y^2$ and $\mathbf{S}$ is the extra stress tensor, defined in the following equation:

$$(1 + \lambda_1^\alpha \frac{D^\alpha}{Dt^\alpha} + \lambda_2^{2\alpha} \frac{D^{2\alpha}}{Dt^{2\alpha}})\mathbf{S} = \mu(1 + \lambda_3^\beta \frac{D^\beta}{Dt^\beta})\mathbf{A}_1, \tag{3}$$

Here, λ_1 and λ_2 represents the relaxation time whereas λ_3 denotes the retardation time,

μ is the dynamic viscosity, and α and β are fractional parameters which satisfy the inequality, $0 \le \alpha \le \beta \le 1$. $\mathbf{A}_1$ is the First Rivlin Erickson tensor and is given by

$$\mathbf{A}_1 = \nabla\mathbf{V} + (\nabla\mathbf{V})^T, \tag{4}$$

and

$$\frac{D^\alpha\mathbf{S}}{Dt^\alpha} = \frac{\tilde{D}^\alpha\mathbf{S}}{\tilde{D}t^\alpha} + (\mathbf{V}\cdot\nabla)\mathbf{S} - (\nabla\mathbf{V})\mathbf{S} - \mathbf{S}(\nabla\mathbf{V})^T, \tag{5}$$

The fractional time derivative of order α with respect to t is given by:

$$\frac{\tilde{D}^\alpha f(t)}{\tilde{D}t^\alpha} = \frac{1}{\Gamma(n-\alpha)}\frac{d}{dt}\int_0^t \frac{f^n(t)}{(t-\xi)^{\alpha-n+1}}d\xi, \quad n-1 < \alpha < n \tag{6}$$

where $\Gamma(.)$ designates the familiar Gamma function. Setting $\alpha = \beta = 1$ in eqn. (3), the fractional Burgers viscoelastic fluid model reduces to the ordinary Burger's viscoelastic model. Further and simpler rheological models may also be extracted from the general eqn. (3). For the case $\lambda_1 = \lambda_2 = 0$ and $\mu\lambda_3 = \alpha_1$, we retrieve the *generalized second grade Reiner-Rivlin viscoelastic model*. With $\lambda_2 = 0 = \lambda_3$, we obtain the *generalized Maxwell viscoelastic fluid model*. Furthermore, for the most elementary case, setting $\lambda_1 = \lambda_2 = \lambda_3 = 0$ and $\alpha = \beta = 1$, and thereby *negating all rheological effects*, the classical *Navier-Stokes* viscous fluid (Newtonian) case is deduced. In the present study we further simulate electrically-conducting fractional Burgers viscoelastic flows. These fluids respond to applied magnetic fields. It is therefore necessary to consider magnetohydrodynamics (MHD). The relevant field equations are the Maxwell equations which fully describe the electromagnetic behavior of fluids and these may be stated following Cramer and Pai [53] and Bég *et al.* [35] in vectorial notation as:

$$\begin{cases} div\mathbf{B} = 0, & \\[2mm] curl\mathbf{B} = \mu_m J, & \\[2mm] curl\mathbf{E} = -\dfrac{\partial\mathbf{B}}{\partial t}, & \\[2mm] J = \sigma_O[\mathbf{E} + \mathbf{V}\times\mathbf{B}] \end{cases} \tag{7}$$

Here $\mathbf{E}$ is electric field vector, μ_m is magnetic permeability of the electro-conductive polymer

(ferrogel), $\boldsymbol{J}$ is the current density and $\boldsymbol{B}$ is the magnetic field vector. Since we have assumed a small magnetic Reynold number, induced magnetic field will be negligible. A single magnetic field component, B_0 acts in the *z*-direction i.e. transverse to the *x-y* plane (the *y*-axis is normal to the *x-z* plane of the diagram). The absence of applied or polarization voltage implies that electrical field effectively vanishes i.e. $\boldsymbol{E} = 0$. Furthermore we neglect Maxwell displacement currents, Hall currents and ionslip effects. In conformity with magnetohydrodynamic conventions, the magnetic lines of force are therefore assumed to be fixed relative to the fluid. Advection is relatively insignificant and therefore the magnetic field is taken as relaxing towards a purely diffusive state, determined by the boundary conditions rather than the flow. Magnetic diffusion greatly exceeds viscous diffusion in the regime. In view of these assumptions we have:

$$\boldsymbol{J} \times \boldsymbol{B} = -\sigma B_0^2 \boldsymbol{V}, \tag{8}$$

To simulate the porous media drag effect, we deploy a modified version of Darcy's law, for a fractional Burger's fluid, wherein the porous resistance (impedance), $\boldsymbol{R}$, satisfies the following relation :

$$\left(1 + \lambda^\alpha \frac{D^\alpha}{Dt^\alpha} + \lambda_2^{2\alpha} \frac{D^{2\alpha}}{Dt^{2\alpha}}\right)\boldsymbol{R} = -\frac{\mu\phi}{k}\left(1 + \lambda_3^\beta \frac{D^\beta}{Dt^\beta}\right)\boldsymbol{V}, \tag{9}$$

Here *k* denotes the permeability and ϕ denotes the porosity of the medium. Implicit in this formulation is the neglection of inertial (second order) drag effects, thermal dispersion and stratification of the porous medium.

3. GENERALIZED MAGNETO-VISCOELASTIC POROUS MEDIA FLOW MODEL

In our analysis, we consider three different problems involving incompressible fractional Burger's viscoelastic magnetohydrodynamic flows. First we derive a generic model for customization to these three cases. We consider flow past an electrically non-conducting rigid plate in a rotating frame of reference. The *z* -axis is orientated perpendicular to the plate i.e. fluid is rotating parallel to the *z* -axis with uniform angular velocity, Ω. Since the plate is infinite in extent, the velocity field will be 2-dimensional (in *x-y* coordinates) and a function only of *z* and *t* independent variables. The fluid has dynamic viscosity, μ. For the velocity field given in Eqn. (3), the continuity equation is identically satisfied and momentum equation in component form is given by the following equations:

$$(1 + \lambda_1^\alpha \frac{\partial^\alpha}{\partial t^\alpha} + \lambda_2^{2\alpha} \frac{\partial^{2\alpha}}{\partial t^{2\alpha}})(\frac{\partial u}{\partial t} - 2\Omega v) = -\frac{1}{\rho}(1 + \lambda_1^\alpha \frac{\partial^\alpha}{\partial t^\alpha} + \lambda_2^{2\alpha} \frac{\partial^{2\alpha}}{\partial t^{2\alpha}})\frac{\partial \hat{p}}{\partial x}$$

$$+ \nu(1 + \lambda_3^\beta \frac{\partial^\beta}{\partial t^\beta})\frac{\partial^2 u}{\partial z^2}$$

$$- \frac{\sigma B_0^2}{\rho}(1 + \lambda_1^\alpha \frac{\partial^\alpha}{\partial t^\alpha} + \lambda_2^{2\alpha} \frac{\partial^{2\alpha}}{\partial t^{2\alpha}})u$$

$$- \frac{\nu\phi}{k}(1 + \lambda_3^\beta \frac{\partial^\beta}{\partial t^\beta})u,$$

(10)

$$(1 + \lambda_1^\alpha \frac{\partial^\alpha}{\partial t^\alpha} + \lambda_2^{2\alpha} \frac{\partial^{2\alpha}}{\partial t^{2\alpha}})(\frac{\partial v}{\partial t} - 2\Omega u) = -\frac{1}{\rho}(1 + \lambda_1^\alpha \frac{\partial^\alpha}{\partial t^\alpha} + \lambda_2^{2\alpha} \frac{\partial^{2\alpha}}{\partial t^{2\alpha}})\frac{\partial \hat{p}}{\partial y}$$

$$+ \nu(1 + \lambda_3^\beta \frac{\partial^\beta}{\partial t^\beta})\frac{\partial^2 v}{\partial z^2}$$

$$- \frac{\sigma B_0^2}{\rho}(1 + \lambda_1^\alpha \frac{\partial^\alpha}{\partial t^\alpha} + \lambda_2^{2\alpha} \frac{\partial^{2\alpha}}{\partial t^{2\alpha}})v$$

$$- \frac{\nu\phi}{k}(1 + \lambda_3^\beta \frac{\partial^\beta}{\partial t^\beta})v,$$

(11)

$$\frac{\partial \hat{p}}{\partial z} = 0,$$

(12)

where ν denotes the kinematic viscosity ($=\mu/\rho$) and $\hat{p}$ denotes the modified pressure, defined thus:

$$\hat{p} = p - (\frac{\rho}{2})\Omega^2 r^2,$$

(13)

Where $p \neq p(z),$ is implied. The coupled (amalgamated) form of Eqn. (10) and Eqn. (11) is given by the following fractional partial differential equation:

$$(1 + \lambda_1^\alpha \frac{\partial^\alpha}{\partial t^\alpha} + \lambda_2^{2\alpha} \frac{\partial^{2\alpha}}{\partial t^{2\alpha}})(\frac{\partial F}{\partial t} + 2i\Omega F)$$

$$= -\frac{1}{\rho}(1 + \lambda_1^\alpha \frac{\partial^\alpha}{\partial t^\alpha} + \lambda_2^{2\alpha} \frac{\partial^{2\alpha}}{\partial t^{2\alpha}})(\frac{\partial \hat{p}}{\partial x} + \iota\frac{\partial \hat{p}}{\partial y})$$

$$+ \nu(1 + \lambda_3^\beta \frac{\partial^\beta}{\partial t^\beta})\frac{\partial^2 F}{\partial z^2} - \frac{\sigma B_0^2}{\rho}(1 + \lambda_1^\alpha \frac{\partial^\alpha}{\partial t^\alpha} + \lambda_2^{2\alpha} \frac{\partial^{2\alpha}}{\partial t^{2\alpha}})F$$

$$- \frac{\nu\phi}{k}(1 + \lambda_3^\beta \frac{\partial^\beta}{\partial t^\beta})F,$$

(14)

where $F = u + iv.$ This denotes the complex variable form of the velocity fields.

4. *CASE I:* **FLOW INDUCED BY GENERAL PERIODIC OSCILLATION**

In this second scenario, we examine flow generated by periodic oscillation at the rigid plate. We further impose the slip condition is defined by the following mathematical expression:

$$u(0,t) - \frac{\gamma}{\mu} S_{xz} = U_0 \sum_{k=-\infty}^{\infty} c_k e^{ik\omega_0 t}, \qquad (15a)$$

$$v(0,t) - \frac{\gamma}{\mu} S_{yz} = 0, \qquad (15b)$$

Here γ is the slip length or slip coefficient and the following free stream velocity conditions are imposed:

$$u, v \to 0 \quad \text{as } z \to \infty. \qquad (15c)$$

The Fourier series coefficients c_k are given by

$$c_k = \frac{1}{T_0} \int_{T_0} f(t) e^{-ik\omega_0 t} dt, \qquad (17)$$

Next we write the boundary conditions in terms of F, giving:

$$(1 + \lambda_1^\alpha \frac{\partial^\alpha}{\partial t^\alpha} + \lambda_2^{2\alpha} \frac{\partial^{2\alpha}}{\partial t^{2\alpha}}) F(z,t) - \gamma(1 + \lambda_3^\beta \frac{\partial^\beta}{\partial t^\beta}) \frac{\partial F}{\partial z}$$

$$= U_0 \sum_{k=-\infty}^{\infty} c_k (1 + \lambda^\alpha \frac{\partial^\alpha}{\partial t^\alpha} + \lambda_2^{2\alpha} \frac{\partial^{2\alpha}}{\partial t^{2\alpha}}) e^{ik\omega_0 t} \quad \text{at} \quad z = 0, \qquad (18)$$

$$F(\infty, t) = 0, \qquad (19)$$

The following non-dimensional quantities are introduced to normalize the boundary value problem, viz:

$$\begin{cases} z^* = \frac{zU_0}{\nu}, & t^* = \frac{tU_0^2}{\nu}, \\[2mm] F^* = \frac{F}{U_0}, & \omega_0^* = \frac{\omega_0\nu}{U_0^2}, \\[2mm] \lambda_1^* = \frac{\lambda_1 U_0^2}{\nu}, & \Omega^* = \frac{\Omega\nu}{U_0^2}, \\[2mm] \lambda_3^* = \frac{\lambda_3 U_0^2}{\nu}, & M^{*2} = \frac{\sigma B_0^2 \nu}{\rho U_0^2}, \\[2mm] \frac{1}{K} = \frac{\phi\nu^2}{kU_0^2}, & \gamma^* = \frac{U_0\gamma}{\nu}, \\[2mm] \lambda_2^* = \frac{\lambda_2 U_0^2}{\nu}, & \end{cases}$$

(19)

Where M^{*2} is the square of the Hartmann magnetohydrodynamic body force parameter, $1/K$ is the inverse permeability parameter, U_o is a reference velocity and ω_0^* is dimensionless angular frequency. All other parameters are dimensionless versions of the original parameter e.g. z^* is dimensionless z-coordinate etc.

The non-dimensional form of eqn. (14) in the absence of pressure gradient is then:

$$(1 + \lambda_1^\alpha \frac{\partial^\alpha}{\partial t^\alpha} + \lambda_2^{2\alpha} \frac{\partial^{2\alpha}}{\partial t^{2\alpha}})(\frac{\partial F}{\partial t} + 2i\Omega F)$$
$$= (1 + \lambda_3^\beta \frac{\partial^\beta}{\partial t^\beta})\frac{\partial^2 F}{\partial z^2} - M^2(1 + \lambda_1^\alpha \frac{\partial^\alpha}{\partial t^\alpha} + \lambda_2^{2\alpha} \frac{\partial^{2\alpha}}{\partial t^{2\alpha}})F$$
$$- \frac{1}{K}(1 + \lambda_3^\beta \frac{\partial^\beta}{\partial t^\beta})F,$$

(20)

The corresponding normalized boundary conditions are:

$$(1 + \lambda_1^\alpha \frac{\partial^\alpha}{\partial t^\alpha} + \lambda_2^{2\alpha} \frac{\partial^{2\alpha}}{\partial t^{2\alpha}})F(z,t) - \gamma(1 + \lambda_3^\beta \frac{\partial^\beta}{\partial t^\beta})\frac{\partial F}{\partial z}$$
$$= \sum_{k=-\infty}^{\infty} c_k(1 + \lambda^\alpha \frac{\partial^\alpha}{\partial t^\alpha} + \lambda_2^{2\alpha} \frac{\partial^{2\alpha}}{\partial t^{2\alpha}})e^{ik\omega_0 t} \quad \text{at} \quad z = 0,$$

(21)

$$F(\infty, t) = 0,$$

(22)

Solving eqn. (20) via implementation of boundary conditions (21) and (22) yields the following series solution:

$$F(z,t) = \sum_{k=-\infty}^{\infty} c_k \left(1 + \lambda_1^\alpha (ik\omega_0)^\alpha + \lambda_2^{2\alpha}(ik\omega_0)^{2\alpha}\right) e^{-m_k z + i(k\omega_0 t - n_k z)}$$

$$\times \left[1/\left((1 + \lambda_1^\alpha (ik\omega_0)^\alpha + \lambda_2^{2\alpha}(ik\omega_0)^{2\alpha}) + \gamma(m_k + in_k)\right. \right.$$

$$\left. \left. (1 + \lambda_3^\beta (ik\omega_0)^\beta)\right)\right],$$

$$(23)$$

$$m_k = \sqrt{\frac{\sqrt{Lr^2 + Li^2} + Lr}{2}}, \quad n_k = \sqrt{\frac{\sqrt{Lr^2 + Li^2} - Lr}{2}},$$

$$(24)$$

$$Lr = \left(\frac{1}{K} + M^2 \left((1 + \lambda^\alpha | k\omega_0 |^\alpha \cos\frac{\alpha\pi}{2} + \lambda_2^{2\alpha}| k\omega_0 |^{2\alpha} \cos\alpha\pi)\right.\right.$$

$$(1 + \lambda_3^\beta | k\omega_0 |^\beta \cos\frac{\beta\pi}{2}) + \lambda_3^\beta (sign(k\omega_0))^2 \sin\frac{\beta\pi}{2}$$

$$(\lambda_1^\alpha | k\omega_0 |^{\alpha+\beta} \sin\frac{\alpha\pi}{2} + \lambda_2^{2\alpha}| k\omega_0 |^{2\alpha+\beta} \sin\alpha\pi))$$

$$-k\omega_0 ((\lambda_1^\alpha | k\omega_0 |^\alpha \sin\frac{\alpha\pi}{2} + \lambda_2^{2\alpha}| k\omega_0 |^{2\alpha} \sin\alpha\pi)$$

$$(1 + \lambda_3^\beta | k\omega_0 |^\beta \cos\frac{\beta\pi}{2}) - \lambda_3^\beta | k\omega_0 |^\beta (sign(k\omega_0)) \sin\frac{\beta\pi}{2}$$

$$(1 + \lambda^\alpha | k\omega_0 |^\alpha \cos\frac{\alpha\pi}{2} + \lambda_2^{2\alpha}| k\omega_0 |^{2\alpha} \cos\alpha\pi))$$

$$-2\Omega ((| k\omega_0 |^\alpha (sign(k\omega_0)) \sin\frac{\alpha\pi}{2} + | k\omega_0 |^{2\alpha}(sign(k\omega_0)) \sin\alpha\pi)$$

$$(1 + \lambda_3^\beta | k\omega_0 |^\beta \cos\frac{\beta\pi}{2}) - \lambda_3^\beta | k\omega_0 |^\beta (sign(k\omega_0)) \sin\frac{\beta\pi}{2}$$

$$(1 + \lambda^\alpha | k\omega_0 |^\alpha \cos\frac{\alpha\pi}{2} + \lambda_2^{2\alpha}| k\omega_0 |^{2\alpha} \cos\alpha\pi)))$$

$$/\left((1 + \lambda_3^\beta | k\omega_0 |^\beta \cos\frac{\beta\pi}{2})^2 + (\lambda_3^\beta | k\omega_0 |^\beta sign(k\omega_0) \sin\frac{\beta\pi}{2})^2\right),$$

$$(25)$$

$$Li = \Big(M^2 \big((\lambda_1^\alpha | k\omega_0 |^\alpha \sin \frac{\alpha\pi}{2} + \lambda_2^{2\alpha} | k\omega_0 |^{2\alpha} \sin \alpha\pi)$$

$$(1 + \lambda_3^\beta | k\omega_0 |^\beta \cos \frac{\beta\pi}{2}) - \lambda_3^\beta | k\omega_0 |^\beta \sin \frac{\beta\pi}{2}$$

$$(1 + \lambda_1^\alpha | k\omega_0 |^\alpha \cos \frac{\alpha\pi}{2} + \lambda_2^{2\alpha} | k\omega_0 |^{2\alpha} \cos \alpha\pi))$$

$$+ \omega \big(1 + (\lambda_1^\alpha | k\omega_0 |^\alpha (sign(k\omega_0)) \cos \frac{\alpha\pi}{2} + \lambda_2^{2\alpha} | k\omega_0 |^{2\alpha}$$

$$(sign(k\omega_0)) \cos \alpha\pi) (1 + \lambda_3^\beta | k\omega_0 |^\beta \cos \frac{\beta\pi}{2})$$

$$- \lambda_3^\beta | k\omega_0 |^\beta \sin \frac{\beta\pi}{2} (1 + \lambda_1^\alpha | k\omega_0 |^\alpha (sign(k\omega_0)) \sin \frac{\alpha\pi}{2}$$

$$+ \lambda_2^{2\alpha} | k\omega_0 |^{2\alpha} \sin \alpha\pi)) + 2\Omega \big(1 + (\lambda_1^\alpha | k\omega_0 |^\alpha$$

$$(sign(k\omega_0)) \cos \frac{\alpha\pi}{2} + \lambda_2^{2\alpha} | k\omega_0 |^{2\alpha} (sign(k\omega_0)) \cos \alpha\pi)$$

$$(1 + \lambda_3^\beta | k\omega_0 |^\beta \cos \frac{\beta\pi}{2}) + \lambda_3^\beta | k\omega_0 |^\beta \sin \frac{\beta\pi}{2} (1 + | k\omega_0 |^\alpha$$

$$(sign(k\omega_0))^2 \sin \frac{\alpha\pi}{2} + | k\omega_0 |^\alpha (sign(k\omega_0))^2 \sin \alpha\pi)) \big)$$

$$/ \Big((1 + \lambda_3^\beta | k\omega_0 |^\beta \cos \frac{\beta\pi}{2})^2 + (\lambda_3^\beta | k\omega_0 |^\beta sign(k\omega_0) \sin \frac{\beta\pi}{2})^2 \Big),$$

$$(26)$$

Solutions have been derived for different oscillations of the plate via the prescription of certain Fourier coefficients, c_k. We select the following five oscillations which refer respectively to exponential, sine-wave, cosine-wave, step and Dirac delta step wave forms:

$$exp(i\omega_0 t), \quad sin(\omega_0 t), \quad cos(\omega_0 t), \quad \begin{cases} 1 & |t| < T_1 \\ 0 & T_1 < |t| < \frac{T_0}{2} \end{cases}, \quad \sum_{k=-\infty}^{\infty} \delta(t - kT_0),$$

$$(27)$$

The following five sets of results are thereby obtained:

$$F_1(z, t) = \big(1 + \lambda_1^\alpha (i\omega_0)^\alpha + \lambda_2^{2\alpha} (i\omega_0)^{2\alpha} \big) e^{-m_1 z + i(\omega_0 t - n_1 z)}$$

$$\times \Big[1 / \big((1 + \lambda_1^\alpha (i\omega_0)^\alpha + \lambda_2^{2\alpha} (i\omega_0)^{2\alpha}) + \gamma(m_1 + in_1)$$

$$(1 + \lambda_3^\beta (i\omega_0)^\beta) \big) \Big],$$

$$(28)$$

$$F_2(z,t) = \frac{1}{2}\left(1 + \lambda_1^\alpha(i\omega_0)^\alpha + \lambda_2^{2\alpha}(i\omega_0)^{2\alpha}\right)e^{-m_1 z + i(\omega_0 t - n_1 z)}$$

$$\times\left[1/\left(\left(1 + \lambda_1^\alpha(i\omega_0)^\alpha + \lambda_2^{2\alpha}(i\omega_0)^{2\alpha}\right)\right.\right.$$

$$\left.\left. + \gamma(m_1 + in_1)\left(1 + \lambda_3^\beta(i\omega_0)^\beta\right)\right)\right]$$

$$+ \frac{1}{2}\left(1 + \lambda_1^\alpha(-i\omega_0)^\alpha + \lambda_2^{2\alpha}(-i\omega_0)^{2\alpha}\right)e^{-m_{-1} z + i(\omega_0 t - n_{-1} z)}$$

$$\times\left[1/\left(\left(1 + \lambda_1^\alpha(-i\omega_0)^\alpha + \lambda_2^{2\alpha}(-i\omega_0)^{2\alpha}\right)\right.\right.$$

$$\left.\left. + \gamma(m_{-1} + in_{-1})\left(1 + \lambda_3^\beta(-i\omega_0)^\beta\right)\right)\right],$$

$$(29)$$

$$F_3(z,t) = \frac{1}{2i}\left(1 + \lambda_1^\alpha(i\omega_0)^\alpha + \lambda_2^{2\alpha}(i\omega_0)^{2\alpha}\right)e^{-m_1 z + i(\omega_0 t - n_1 z)}$$

$$\times\left[1/\left(\left(1 + \lambda_1^\alpha(i\omega_0)^\alpha + \lambda_2^{2\alpha}(i\omega_0)^{2\alpha}\right)\right.\right.$$

$$\left.\left. + \gamma(m_1 + in_1)\left(1 + \lambda_3^\beta(i\omega_0)^\beta\right)\right)\right]$$

$$- \frac{1}{2i}\left(1 + \lambda_1^\alpha(-i\omega_0)^\alpha + \lambda_2^{2\alpha}(-i\omega_0)^{2\alpha}\right)e^{-m_{-1} z + i(\omega_0 t - n_{-1} z)}$$

$$\times\left[1/\left(\left(1 + \lambda_1^\alpha(-i\omega_0)^\alpha + \lambda_2^{2\alpha}(-i\omega_0)^{2\alpha}\right)\right.\right.$$

$$\left.\left. + \gamma(m_{-1} + in_{-1})\left(1 + \lambda_3^\beta(-i\omega_0)^\beta\right)\right)\right],$$

$$(30)$$

$$F_4(z,t) = \sum_{k=-\infty}^{\infty}\left(\frac{\sin(k\omega_0 T_1)}{k\pi}\right)\left(1 + \lambda^\alpha(ik\omega_0)^\alpha\right.$$

$$\left. + \lambda_2^{2\alpha}(i\omega_0)^{2\alpha}\right)e^{-m_k z + i(k\omega_0 t - n_k z)}$$

$$\times\left[1/\left(\left(1 + \lambda^\alpha(ik\omega_0)^\alpha + \lambda_2^{2\alpha}(i\omega_0)^{2\alpha}\right) + \gamma(m_k + in_k)\right.\right.$$

$$\left.\left.\left(1 + \lambda_3^\beta(ik\omega_0)^\beta\right)\right)\right],$$

$$(31)$$

$$F_5(z,t) = \frac{1}{T_0} \sum_{k=-\infty}^{\infty} \left(1 + \lambda^\alpha (ik\omega_0)^\alpha \right.$$

$$+ \lambda_2^{2\alpha}(i\omega_0)^{2\alpha}\Big) e^{-m_k z + i(k\omega_0 t - n_k z)}$$

$$\times \left[1/\Big(\big(1 + \lambda^\alpha(ik\omega_0)^\alpha + \lambda_2^{2\alpha}(i\omega_0)^{2\alpha}\big) + \gamma(m_k + in_k) \right.$$

$$\left. \big(1 + \lambda_3^\beta(ik\omega_0)^\beta\big)\Big) \right].$$

(32)

All five oscillatory cases pertaining to Case I are elaborated upon in due course.

5. *CASE II*: PERIODIC FLOW BETWEEN TWO RIGID PLATES

A generic geometrical representation for this case is illustrated in **Fig. 1** below. Let us know consider flow between two plates which are rigid i.e. a parallel plate channel (this geometry is more relevant to MHD energy generator systems whereas the scenario in Case I is more relevant to sheet processing of ferrogels). The channel depth is h i.e. the plates are separated by a distance h. The appropriate non-dimensional equation is as follows:

$$(1 + \lambda_1^\alpha \frac{\partial^\alpha}{\partial t^\alpha} + \lambda_2^{2\alpha} \frac{\partial^{2\alpha}}{\partial t^{2\alpha}})(\frac{\partial F}{\partial t} + 2i\Omega F)$$

$$= (1 + \lambda_3^\beta \frac{\partial^\beta}{\partial t^\beta})\frac{\partial^2 F}{\partial z^2} - M^2(1 + \lambda_1^\alpha \frac{\partial^\alpha}{\partial t^\alpha} + \lambda_2^{2\alpha} \frac{\partial^{2\alpha}}{\partial t^{2\alpha}})F$$

$$- \frac{1}{K}(1 + \lambda_3^\beta \frac{\partial^\beta}{\partial t^\beta})F,$$

(33)

The associated boundary conditions are:

$$(1 + \lambda_1^\alpha \frac{\partial^\alpha}{\partial t^\alpha} + \lambda_2^{2\alpha} \frac{\partial^{2\alpha}}{\partial t^{2\alpha}})F(z,t) - \gamma(1 + \lambda_3^\beta \frac{\partial^\beta}{\partial t^\beta})\frac{\partial F}{\partial z}$$

$$= \sum_{k=-\infty}^{\infty} c_k (1 + \lambda_1^\alpha \frac{\partial^\alpha}{\partial t^\alpha} + \lambda_2^{2\alpha} \frac{\partial^{2\alpha}}{\partial t^{2\alpha}})e^{ik\omega_0 t} \quad \text{at} \quad z = 0,$$

(34)

$$(1 + \lambda_1^\alpha \frac{\partial^\alpha}{\partial t^\alpha} + \lambda_2^{2\alpha} \frac{\partial^{2\alpha}}{\partial t^{2\alpha}})F(z,t) + \gamma(1 + \lambda_3^\beta \frac{\partial^\beta}{\partial t^\beta})\frac{\partial F}{\partial z} = 0 \quad \text{at} \quad z = 1,$$

(35)

By the help of Fourier transforms the following solution is attained:

$$
\begin{aligned}
F(z,t) = \sum_{k=-\infty}^{\infty} & c_k \left(1+\lambda^\alpha (ik\omega_0)^\alpha + \lambda_2^{2\alpha}(ik\omega_0)^{2\alpha}\right)^2 \sinh l_k (1-z) \\
& + \gamma\left(1+\lambda^\alpha (ik\omega_0)^\alpha + \lambda_2^{2\alpha}(ik\omega_0)^{2\alpha}\right)\left(1+\lambda_3^\beta (ik\omega_0)^\beta\right) \\
& l_k \cosh l_k (1-z) \times \left[1/\left(\left(1+\lambda^\alpha (ik\omega_0)^\alpha + \lambda_2^{2\alpha}(ik\omega_0)^{2\alpha}\right)\right.\right. \\
& \left(2\gamma\left(1+\theta^\beta (ik\omega_0)^\beta l_k \cosh l_k + \left(1+\lambda^\alpha (ik\omega_0)^\alpha\right.\right.\right. \\
& \left.\left.\left.+ \lambda_2^{2\alpha}(ik\omega_0)^{2\alpha}\right) \sinh l_k\right) + \gamma^2 \left(1+\lambda_3^\beta (ik\omega_0)^\beta\right)^2 l_k^2 \sinh l_k \right) \Big] e^{ik\omega_0 t},
\end{aligned}
\tag{36}
$$

where

$$
\begin{aligned}
l_k^2 = \frac{1}{1+\lambda_3^\beta (ik\omega_0)^\beta} & \left[M^2\left(1+\lambda_1^\alpha (ik\omega_0)^\alpha + \lambda_2^{2\alpha}(ik\omega_0)^{2\alpha}\right) + \frac{1}{K}\left(1+\lambda_3^\beta (ik\omega_0)^\beta\right) \right. \\
& \left. + i(k\omega_0 + 2\Omega)\left(1+\lambda_1^\alpha (ik\omega_0)^\alpha + \lambda_2^{2\alpha}(ik\omega_0)^{2\alpha}\right) \right],
\end{aligned}
\tag{37}
$$

The solutions for the five oscillation cases (as stated in Case I) for the present scenario emerge as:

$$
\begin{aligned}
F_1(z,t) = & \left(\left(1+\lambda_1^\alpha (i\omega_0)^\alpha + \lambda_2^{2\alpha}(ik\omega_0)^{2\alpha}\right)^2 \sinh l_1(1-z)\right. \\
& + \gamma\left(1+\lambda_1^\alpha (i\omega_0)^\alpha + \lambda_2^{2\alpha}(ik\omega_0)^{2\alpha}\right)\left(1+\lambda_3^\beta (i\omega_0)^\beta\right) \\
& \left. l_1 \cosh l_1(1-z)\right) \times \left[1/\left(2\gamma\left(1+\lambda_3^\beta (i\omega_0)^\beta\right)\right.\right. \\
& \left(1+\lambda_1^\alpha (i\omega_0)^\alpha + \lambda_2^{2\alpha}(ik\omega_0)^{2\alpha}\right) l_1 \cosh l_1 \\
& + \left(\gamma^2\left(1+\lambda_3^\beta (i\omega_0)^\beta\right)^2 l_1^2 + \left(1+\lambda_1^\alpha (i\omega_0)^\alpha\right.\right. \\
& \left.\left.\left.+ \lambda_2^{2\alpha}(ik\omega_0)^{2\alpha}\right)^2\right) \sinh l_1\right) \Big],
\end{aligned}
\tag{38}
$$

$$F_2(z,t) = \frac{1}{2}\Big[\Big((1+\lambda_1^\alpha(i\omega_0)^\alpha+\lambda_2^{2\alpha}(ik\omega_0)^{2\alpha})^2\sinh l_1(1-z)$$

$$+\gamma(1+\lambda_1^\alpha(i\omega_0)^\alpha+\lambda_2^{2\alpha}(ik\omega_0)^{2\alpha})l_1\cosh l_1(1-z)$$

$$(1+\lambda_3^\beta(i\omega_0)^\beta)\Big)\times\Big(1/(2\gamma(1+\lambda_3^\beta(i\omega_0)^\beta)$$

$$(1+\lambda_1^\alpha(i\omega_0)^\alpha+\lambda_2^{2\alpha}(ik\omega_0)^{2\alpha})l_1\cosh l_1$$

$$+(\gamma^2(1+\lambda_3^\beta(i\omega_0)^\beta)^2l_1^2+(1+\lambda_1^\alpha(i\omega_0)^\alpha$$

$$+\lambda_2^{2\alpha}(ik\omega_0)^{2\alpha})^2)\sinh l_1)\Big)e^{i\omega_0 t}$$

$$+\Big((1+\lambda_1^\alpha(-i\omega_0)^\alpha+\lambda_2^{2\alpha}(ik\omega_0)^{2\alpha})^2\sinh l_{-1}(1-z)$$

$$+\gamma(1+\lambda_1^\alpha(-i\omega_0)^\alpha+\lambda_2^{2\alpha}(ik\omega_0)^{2\alpha})l_{-1}\cosh l_{-1}(1-z)$$

$$(1+\lambda_3^\beta(-i\omega_0)^\beta)\Big)\times\Big(1/(2\gamma(1+\lambda_3^\beta(-i\omega_0)^\beta)$$

$$(1+\lambda_1^\alpha(-i\omega_0)^\alpha+\lambda_2^{2\alpha}(ik\omega_0)^{2\alpha})l_{-1}\cosh l_{-1}$$

$$+(\gamma^2(1+\lambda_3^\beta(-i\omega_0)^\beta)^2l_{-1}^2+(1+\lambda_1^\alpha(-i\omega_0)^\alpha$$

$$+\lambda_2^{2\alpha}(ik\omega_0)^{2\alpha})^2)\sinh l_{-1})\Big)e^{-i\omega_0 t}\Big],$$

(39)

$$F_3(z,t) = \frac{1}{2i}\Big[\Big((1+\lambda_1^\alpha(i\omega_0)^\alpha+\lambda_2^{2\alpha}(ik\omega_0)^{2\alpha})^2\sinh l_1(1-z)$$

$$+\gamma(1+\lambda_1^\alpha(i\omega_0)^\alpha+\lambda_2^{2\alpha}(ik\omega_0)^{2\alpha})l_1\cosh l_1(1-z)$$

$$(1+\lambda_3^\beta(i\omega_0)^\beta)\Big)\times\Big(1/(2\gamma(1+\lambda_3^\beta(i\omega_0)^\beta)$$

$$(1+\lambda_1^\alpha(i\omega_0)^\alpha+\lambda_2^{2\alpha}(ik\omega_0)^{2\alpha})l_1\cosh l_1$$

$$+(\gamma^2(1+\lambda_3^\beta(i\omega_0)^\beta)^2l_1^2+(1+\lambda_1^\alpha(i\omega_0)^\alpha$$

$$+\lambda_2^{2\alpha}(ik\omega_0)^{2\alpha})^2)\sinh l_1)\Big)e^{i\omega_0 t}$$

$$-\Big((1+\lambda_1^\alpha(-i\omega_0)^\alpha+\lambda_2^{2\alpha}(ik\omega_0)^{2\alpha})^2\sinh l_{-1}(1-z)$$

$$+\gamma(1+\lambda_1^\alpha(-i\omega_0)^\alpha+\lambda_2^{2\alpha}(ik\omega_0)^{2\alpha})l_{-1}\cosh l_{-1}(1-z)$$

$$(1+\lambda_3^\beta(-i\omega_0)^\beta)\Big)\times\Big(1/(2\gamma(1+\lambda_3^\beta(-i\omega_0)^\beta)$$

$$(1+\lambda_1^\alpha(-i\omega_0)^\alpha+\lambda_2^{2\alpha}(ik\omega_0)^{2\alpha})l_{-1}\cosh l_{-1}$$

$$+(\gamma^2(1+\lambda_3^\beta(-i\omega_0)^\beta)^2l_{-1}^2+(1+\lambda_1^\alpha(-i\omega_0)^\alpha$$

$$+\lambda_2^{2\alpha}(ik\omega_0)^{2\alpha})^2)\sinh l_{-1})\Big)e^{-i\omega_0 t}\Big],$$

(40)

$$F_4(z,t) = \sum_{k=-\infty}^{\infty} \frac{\sin(k\omega_0 T_1)}{k\pi} \Big(\big(1 + \lambda_1^\alpha (ik\omega_0)^\alpha$$

$$+ \lambda_2^{2\alpha}(ik\omega_0)^{2\alpha}\big)^2 \sinh l_k (1-z) + \gamma \big(1 + \lambda_1^\alpha (ik\omega_0)^\alpha$$

$$+ \lambda_2^{2\alpha}(ik\omega_0)^{2\alpha}\big)\big(1 + \lambda_3^\beta (ik\omega_0)^\beta\big)l_k \cosh l_k (1-z) \Big)$$

$$\times \Big[1/\big(2\gamma\big(1 + \lambda_1^\alpha (ik\omega_0)^\alpha + \lambda_2^{2\alpha}(ik\omega_0)^{2\alpha}\big)$$

$$\big(1 + \lambda_3^\beta (ik\omega_0)^\beta\big)l_k \cosh l_k + \big(\gamma^2 \big(1 + \lambda_3^\beta (ik\omega_0)^\beta\big)^2 l_k^2$$

$$+ \big(1 + \lambda_1^\alpha (ik\omega_0) + \lambda_2^{2\alpha}(ik\omega_0)^{2\alpha}\big)^2\big)\sinh l_k \Big) \Big] e^{ik\omega_0 t}, \tag{41}$$

$$F_5(z,t) = \frac{1}{T_0} \sum_{k=-\infty}^{\infty} \Big(\big(1 + \lambda_1^\alpha (ik\omega_0)^\alpha + \lambda_2^{2\alpha}(ik\omega_0)^{2\alpha}\big)^2 \sinh l_k (1-z)$$

$$+ \gamma \big(1 + \lambda_1^\alpha (ik\omega_0)^\alpha + \lambda_2^{2\alpha}(ik\omega_0)^{2\alpha}\big)l_k \cosh l_k (1-z) \Big)$$

$$\big(1 + \lambda_3^\beta (ik\omega_0)^\beta\big) \times \Big[1/\big(2\gamma\big(1 + \lambda_1^\alpha (ik\omega_0)^\alpha + \lambda_2^{2\alpha}(ik\omega_0)^{2\alpha}\big) \tag{42}$$

$$\big(1 + \lambda_3^\beta (ik\omega_0)^\beta\big)l_k \cosh l_k + \big(\gamma^2 \big(1 + \lambda_3^\beta (ik\omega_0)^\beta\big)^2 l_k^2$$

$$+ \big(1 + \lambda_1^\alpha (ik\omega_0) + \lambda_2^{2\alpha}(ik\omega_0)^{2\alpha}\big)^2\big)\sinh l_k \Big) \Big] e^{ik\omega_0 t}.$$

6. *CASE III*: **POISEUILLE FLOW**

We consider finally the Poiseuille channel flow version of the generalized model given in section 3. This case is of fundamental importance in MHD generator flows. Both channel plates are stationary, infinite in length and separated by a distance *2h*. The flow is generated due to the pressure gradient, which is given as:

$$\frac{\partial \hat{p}}{\partial x} + i\frac{\partial \hat{p}}{\partial y} = \rho Q_0 e^{i\omega_0 t}, \tag{43}$$

The associated non-dimensional problem for this scenario takes the form:

$$\big(1 + \lambda_1^\alpha \frac{\partial^\alpha}{\partial t^\alpha} + \lambda_2^{2\alpha}\frac{\partial^{2\alpha}}{\partial t^{2\alpha}}\big)\big(\frac{\partial F}{\partial t} + 2i\Omega F\big)$$

$$= -\big(1 + \lambda_1^\alpha \frac{\partial^\alpha}{\partial t^\alpha} + \lambda_2^{2\alpha}\frac{\partial^{2\alpha}}{\partial t^{2\alpha}}\big)Q_0 e^{i\omega_0 t} + \big(1 + \lambda_3^\beta \frac{\partial^\beta}{\partial t^\beta}\big)\frac{\partial^2 F}{\partial z^2} \tag{44}$$

$$-M^2\big(1 + \lambda_1^\alpha \frac{\partial^\alpha}{\partial t^\alpha} + \lambda_2^{2\alpha}\frac{\partial^{2\alpha}}{\partial t^{2\alpha}}\big)F - \frac{1}{K}\big(1 + \lambda_3^\beta \frac{\partial^\beta}{\partial t^\beta}\big)F,$$

$$\left(1+\lambda_1^\alpha\frac{\partial^\alpha}{\partial t^\alpha}+\lambda_2^{2\alpha}\frac{\partial^{2\alpha}}{\partial t^{2\alpha}}\right)F(z,t)+\gamma\left(1+\lambda_3^\beta\frac{\partial^\beta}{\partial t^\beta}\right)\frac{\partial F}{\partial z}=0 \quad \text{at} \quad z=1, \tag{45}$$

$$\left(1+\lambda_1^\alpha\frac{\partial^\alpha}{\partial t^\alpha}+\lambda_2^{2\alpha}\frac{\partial^{2\alpha}}{\partial t^{2\alpha}}\right)F(z,t)-\gamma\left(1+\lambda_3^\beta\frac{\partial^\beta}{\partial t^\beta}\right)\frac{\partial F}{\partial z}=0 \quad \text{at} \quad z=-1, \tag{46}$$

The solution of Eq. (42) subject to boundary conditions (45) and (46) is given by:

$$\begin{aligned}
F(z,t)=Q_0 &\left(\frac{1+\lambda_1^\alpha(i\omega_0)^\alpha+\lambda_2^{2\alpha}(i\omega_0)^{2\alpha}}{1+\lambda_3^\beta(i\omega_0)^\beta}\right)\Big[\left(\cosh l_k z-\cosh l_k\right)\\
&\left(1+\lambda_1^\alpha(i\omega_0)^\alpha+\lambda_2^{2\alpha}(i\omega_0)^{2\alpha}\right)-\gamma\left(1+\lambda_3^\beta(i\omega_0)^\beta\right)\\
&l_k\sinh l_k\Big]\times\Big[1/\Big(l_k^2\big(\gamma\left(1+\lambda_3^\beta(i\omega_0)^\beta\right)l_k\sinh l_k\\
&+\left(1+\lambda_1^\alpha(i\omega_0)^\alpha+\lambda_2^{2\alpha}(i\omega_0)^{2\alpha}\right)\cosh l_k\big)\Big)\Big]e^{i\omega_0 t},
\end{aligned} \tag{47}$$

$$l_1=l_k\,|_{k=1}. \tag{48}$$

7. GRAPHICAL RESULTS AND DISCUSSION

Extensive graphical plots and Tables have been presented for the solutions described above. In **Tables 1-6** the analytical solutions for *u* and *v* i.e. x- and y-components of the velocity field have been presented both with slip (Tables 1-3) and without slip (Tables 4-6), for each Case studied. In all the tables, the oscillation imposed at the plate (s) is of the *cosω_0t* waveform. In each of the Tables 1-6, five material models are studied i.e. *Newtonian, generalized (G.) Maxwell, generalized (G.) Oldroyd-B model, Burger's model and the fractional Burger's model*. We do not explicitly study the influence of a porous medium and *K* is prescribed as unity i.e. $1/K=1$ corresponding to a highly permeable medium. Furthermore we do not explicitly investigate the influence of rotational parameter (Ω) which is fixed at 0.3 throughout all computations. The elucidation of Coriolis forces on the regime is deferred to a future article. Also the magnetic field strength is not studied i.e. a constant *M* value of 0.5 is imposed and angular oscillation frequency and time coordinate are also fixed at 0.1 and 0.5 respectively. Comparing the tables (e.g. Table 1 compared with Table 4, Table 2 compared with Table 5 and Table 3 compared with Table 6) allows an assessment of the *influence of wall hydrodynamic slip* on both velocity components. With slip present lower magnitudes of *u*-velocity (primary) component are observed for all five types of

fluid material model. However for the secondary v-velocity component, higher values are computed for the four non-Newtonian models when slip is present (Tables 1-3) compared with when slip is absent (Tables 4-6). Only the Newtonian model achieves higher v-velocity values without slip than with slip present. Evidently therefore the presence of slip *decelerates* the primary flow irrespective of the material model, whereas it *accelerates* the secondary flow for rheological fluids only. An implication of this in MHD generators is that greater efficiency can be achieved in the secondary flow field with wall slip whereas losses are incurred in the primary flow with wall slip, when the working fluid is non-Newtonian. We note that in all cases the primary flow is positive whereas the secondary flow is negative indicating that backflow is induced in the latter, a characteristic of real MHD energy generator flows. This concurs with the observations of Fabris and Hantman [36]. With regard to the influence of material model on velocity distributions, it is apparent from inspection of the slip case Tables (i.e. Tables 1-3) that both primary and secondary velocity components are maximized for the generalized Maxwell rheological model (G. Maxwell) whereas in Tables 1 and 2 (i.e. for Cases I and II) they are minimized for the Burger's fluid model. However in Table 3 the minimum primary velocity is in fact computed for the Newtonian fluid whereas the minimum magnitude of secondary velocity corresponds as in Tables 1 and 2, to the Burger's fluid case. Evidently the nature of the flow regime combined with the selection of material model has an important collective influence on the efficiency of the flow. Overall the fractional Burger's viscoelastic model is also found to achieve significantly greater primary and secondary velocity magnitudes than the conventional Burger's fluid model. The incorporation of fractional calculus in the Burger's model is therefore not a futile exercise and demonstrates non-trivial rheological effects. Considering the no-slip solutions (Tables 4-6), a very different response is computed from the slip solutions (Tables 1-3). Whereas in the latter the primary velocity minima generally correspond to the Burger's fluid, in the former (no-slip cases) the primary velocity peak (maximum) is associated with the Burger's model, for Cases I and II; however in Case III (Pouiseille flow) the maximum primary velocity is computed for the generalized Maxwell model (as with Tables 1-3 for slip solutions). The minimum primary velocity magnitudes are found to be attained with the Newtonian model in Tables 4 and 5 but again with the Burger's model in Tables 6 (Case III). Effectively Table 4 shows that primary (u-) velocity is a maximum in the Burger's fluid model and minimum in the Newtonian model. The fractional Burger's fluid therefore achieves a lower primary velocity than the Burger's fluid model. Secondary velocity is a maximum in the

Burger's fluid and attains the least value in the fractional Burger's model. Table 5 demonstrates that the primary velocity (*u-component*) magnitude is greater in the Burger's fluid model than the fractional Burger's model and a similar trend is observed for the secondary velocity (*v-component*). Finally Table 6 (corresponding to Case III- Poisuille flow) shows that primary velocity magnitude is maximum for the generalized Maxwell fluid, whereas secondary velocity is maximum for the conventional Burger's fluid (i.e. lowest negative value). The fractional Burger's fluid achieves a greater primary velocity than the conventional Burger's fluid, whereas the conventional Burger's fluid model attains a higher maximum secondary velocity than the fractional Burger's model.

Figs 2-4 illustrate the graphical distributions of both primary and secondary velocity components for all five material models, for each Case examined. These are plotted to investigate slip (γ) effect and also rheological parameter effects (i.e. α, β, λ_1, λ_2, λ_3) via the different material models). **Fig 2** shows the effect of slip parameter γ for Case 1 i.e. *general periodic oscillation in magneto-viscoelastic flow from a rigid non-conducting plate*. With greater slip there is a significant deceleration in primary velocity for all five material models. However with greater slip parameter, the secondary velocity field is initially decelerated for small values of *z*, and thereafter it is markedly accelerated with increasing slip, for all five material models. Although the trends are similar for all five material models, there is a large deviation in magnitudes indicating that the selection of material model influences the maximum and minimum values of primary and secondary velocity, rather than the nature of the response, which is more dominated by the type of flow regime i.e. periodic oscillation from a non-conducting plate. These observations are consistent with the earlier literature on rotating magnetohydrodynamic oscillatory flows e.g. Zheng *et al*. [39] and Khan and Khan [45] i.e. monotonic decays are consistently computed for primary velocity with strongly skewed parabolic distributions (biased towards the lower values of *z*) for secondary velocity. **Fig. 3** shows the effect of slip parameter (γ) on primary and secondary velocity components, for Case II i.e. periodic magneto-viscoelastic flow between two plates (flow under an imposed cosine waveform $\cos\omega_0 t$). Here it is apparent immediately that very different profiles are computed compared to Case I. The primary velocity plots are generally linear decays whereas the secondary velocity plots are more evenly distributed parabolas. For all five material models, the primary velocity initially decreases strongly with increasing slip, and then at intermediate values of z the reverse trend arises i.e. thereafter primary velocity ascends with greater

slip. This indicates that the slip effect is decelerating close to the plates but this effect is weakened further from them i.e. towards the core region of the channel flow. This effect has also been observed in real MHD channel flows as elaborated by Sutton and Sherman [54] and Rosa [55]. Secondary velocity is observed to be maximized at the channel walls (z=0, 1) whereas it is minimized in the core region, for all five fluid models. With increasing slip there is a substantial deceleration in the secondary flow across the channel width. There is also a slight skewness in the secondary profiles towards the lower channel wall ($z = 0$). **Fig. 4** depicts the influence of slip parameter for Case III i.e. *Poiseuille flow under a pressure gradient*. While secondary velocity distributions are similar to Case II (channel flow) the primary velocity plots are significantly different from both Case I and II since they are now inverted parabolas which are approximately symmetric about the channel centre line (z=0.5). The maximum primary velocity always arises at the channel centre whereas the secondary velocity is always a minimum at that location (it is maximized at the channel walls). With increasing slip primary velocity is significantly accelerated whereas secondary velocity is decelerated, and these patterns are sustained across the channel width, for all five materials models. As eludicated earlier, the generalized Maxwell model attains the maximum primary velocity, indicating that the presence of fractional and relaxation parameters ($\alpha, \beta, \lambda_1, \lambda_2$ *are all non-zero)* and the simultaneous absence of the rheological retardation parameter (λ_3=0) has a beneficial effect on the *primary flow*. Conversely however the generalized Maxwell model also achieves the minimum secondary velocity values.

8. CONCLUSIONS

A generalized mathematical model is developed for hydromagnetic flows of incompressible fractional Burger's viscoelastic fluid via a porous medium in a rotating frame of reference with wall slip effects. The fractional generalized Darcy model is utilized to model porous medium bulk drag force effects. Three different cases are derived from the general non-dimensional mathematical model - namely, case I -flow induced by a general periodic oscillation at a rigid plate, Case II -periodic flow in a parallel plate channel and finally Case III-Poiseuille flow. In all cases the plate (s) boundary (ies) are electrically-non-conducting and magnetic induction effects are neglected. The well-posed boundary value problems associated with each case are solved via Fourier transforms. Comparisons are made between the results derived with and without slip conditions. 4 special cases are retrieved from the general fractional Burgers model, viz *Newtonian*

fluid, general Maxwell viscoelastic fluid, generalized Oldroyd-B fluid and the conventional Burger's viscoelastic model. The computations reveal that both material model selected and the nature of the flow problem exert a significant influence on primary and secondary velocity fields. The presence of slip is observed to accelerate the primary flow in Case III, whereas it consistently decelerates the primary flow in Case I and initially decelerates and thereafter accelerates the primary flow in Case II. Conversely increasing wall slip is observed to initially decelerate secondary velocity and then accelerate it for Case I, whereas it consistently decelerates the secondary flow for both Cases I and II. The results computed also illustrate that primary velocity (*u-component*) magnitude in Case II, for the Burger's fluid model exceeds that for the fractional Burger's model and a similar trend is observed for the secondary velocity (*v-component*). It is also noteworthy that for Case III (Poiseuille flow) primary velocity magnitude is greatest for the generalized Maxwell fluid, whereas secondary velocity is a maximum for the conventional Burger's fluid. In this scenario (Case III) the fractional Burger's fluid attains a greater primary velocity than the conventional Burger's fluid, whereas the conventional Burger's fluid model attains a higher maximum secondary velocity than the fractional Burger's model. The present study provides a useful benchmark for further (numerical) investigations. It is relevant to fluid dynamic processes in MHD rotating energy generators employing rheological working fluids, and although many non-Newtonian models have been addressed, the influence of micro-structure has been neglected. This feature is best addressed with Eringen micro-continuum (e.g. micropolar) models [56] and efforts in this regard are underway and will be communicated imminently.

REFERENCES

[1] Suryawanshi SS, Kunjwani HK, KawadeJayashree V, AlkunteMohita A, Yadav Dattatraya J. Novel polymeric in situ gels for ophthalmic drug delivery system, *J. Advanced Pharmaceutical Technology & Research*., 2, 67–83 (2012).

[2] N.J. Balmforth and R.V. Craster A consistent thin-layer theory for Bingham plastics, *J. Non-Newtonian Fluid Mech*., 84, 65-81 (1999).

[3] Ver Strate, G. and Struglinski, M.J., Polymers as lubricating-oil viscosity modifiers. In: *Polymers as Rheology Modifiers, Proceedings of the ACS Symposium Series, 462, American Chemical Society*, 256-272 (1991).

[4] Jokuty, P., M. Fingas, S. Whiticar, and B. Fieldhouse, A study of viscosity and interfacial

tension of oils and emulsions, *Environment Canada Manuscript Report Number EE-153, Ottawa, Ontario*, 43 pp (1995).

[5] R.P. Chhabra and J.F. Richardson, *Non-Newtonian Flow and Applied Rheology, Engineering Applications*, 2nd edn, Elsevier, New York (2008).

[6] F. Irgens, *Rheology and Non-Newtonian Fluids,* Springer, Berlin (2014).

[7] D.D. Joseph, *Fluid Dynamics of Viscoelastic Liquids*, Springer, New York (1990).

[8] M.J. Crochet and R. Keunings, Die swell of a Maxwell fluid - numerical prediction*, J. Non-Newtonian Fluid Mech.*, 7, 199-212 (1980).

[9] Jamil, M., Fetecau, C., and Imran, M. Unsteady helical flows of Oldroyd-B fluids, *Comm. Nonlinear Science and Numerical Simulation*, 16(3), 1378–1386 (2011).

[10] T. Sarpkaya and P.G. Rainey, Stagnation point flow of a second-order viscoelastic fluid, *Acta Mechanica*, 11, 237-246 (1971).

[11] B. Sahoo, S. Poncet, Flow and heat transfer of third grade fluid past an exponentially stretching sheet with partial slip boundary conditions, *Int. J. Heat and Mass Transfer*, 54, 23-24, 5010-5019 (2011).

[12] V. R. Prasad, S. Abdul Gaffar, E. Keshava Reddy and O. Anwar Beg, Flow and heat transfer of Jeffery's non-Newtonian fluid from horizontal circular cylinder, *AIAA J. Thermophysics Heat Transfer*, 28(4), 764-770 (2014).

[14] Akbar Zaman, Nasir Ali and O. Anwar Bég, Numerical study of unsteady blood flow through a vessel using Sisko model, *Engineering Science and Technology-An International Journal,* 10 pages (2015). DOI: 10.1016/J.JESTCH.2015.09.013

[15] D. Tripathi and O. Anwar Bég, Peristaltic propulsion of generalized Burgers' fluids through a non-uniform porous medium: A study of chyme dynamics through the intestine, *Mathematical Biosciences* 248:67-77 (2014).

[16] Scott Blair, G. W., Veinoglou, B. C., and Caffyn, J. E., Limitations of the Newtonian time scale in relation to non-equilibrium rheological states and a theory of quasi-properties, *Proc. R. Soc. London, Ser. A*, 187, 69– 85 (1947).

[17] Graham, A., Scott Blair, G. W. and Withers, R. F. J., A methodological problem in rheology, *British J. Philosophical Science*, 11, 265–27 (1961).

[18] Z. Lei, C. Liu, and Y. Zhou, Global solutions for incompressible viscoelastic fluids, *Archive for Rational Mechanics and Analysis*, 188, 371-398 (2008).

[19] F. Lin, C. Liu, and P. Zhang, On hydrodynamics of viscoelastic fluids, *Comm. Pure and Applied Mathematics* 58, 1437-1471 (2005).

[20] S. Wang and M. Xu, Axial Couette flow of two kinds of fractional viscoelastic fluids in an annulus, *Nonlinear Analysis: Real World Applications*, 10, 1087-1096 (2009).

[21] D.K. Tong and Y.S. Liu, Exact solutions for the unsteady rotational flow of non-Newtonian fluid in an annular pipe, *Int. J. Eng. Sci.* 43, 281-289 (2005).

[22] M. Khan, S.H. Ali, and H.T. Qi, Exact solutions of starting flows for a fractional Burger's fluid between coaxial cylinders, *Nonlinear Analysis: Real World Applications,* 10, 1775-1783 (2009).

[23] Bagley, R. L., Torvik, P. J., On the fractional calculus model of viscoelastic behavior, *J. Rheology,* 30, 133-155 (1986).

[24] D.Y. Song, T.Q. Jiang, Study on the constitutive equation with fractional derivative for the viscoelastic fluids – modified Jeffreys model and its application, *Rheol. Acta*, 37, 512–517 (1998).

[25] R. Hilfer, *Applications of Fractional Calculus in Physics*, World Scientific Press, Singapore, (2000).

[26] H. Qi and M. Xu, Some unsteady unidirectional flows of a generalized Oldroyd-B fluid with fractional derivative, *Applied Mathematical Modelling,* 33, 4184–4191 (2009).

[27] H. Qi and H. Jin, Unsteady helical flows of a generalized Oldroyd-B fluid with fractional derivative, *Nonlinear Analysis: Real World Applications*, 10, 2700-2708 (2009).

[28] M. Mooney, Explicit formulas for slip and fluidity, *J. Rheology*, 2, 210-222 (1931).

[29] V. Bertola, A note on the effects of liquid viscoelasticity and wall slip on foam drainage, *J. Physics: Condensed Matter,* 19, 110-120 (2007).

[30] M. M. Mohseni and F. Rashidi, Axial annular flow of a Giesekus fluid with wall slip above the critical shear stress, *J. Non-Newtonian Fluid Mechanics*, 223 (2015). DOI: j.jnnfm. 2015.05.004

[31] S. Abelman, E. Momoniat, and T. Hayat, Couette flow of a third grade fluid with rotating frame and slip condition, *Nonlinear Analysis: Real World Applications* 10 (2009), 3329-3334

[32] D. Tripathi, O. Anwar Bég and J. Curiel-Sosa, Homotopy semi-numerical simulation of peristaltic flow of generalized Oldroyd-B fluids with slip effects, *Computer Methods in Biomechanics Biomedical Engineering,* 17(4) 433-442 (2014).

[33] Y. Han, Mechanics of magneto-active polymers, *PhD Thesis, Engineering Mechanics, Iowa State University, USA* (2012).

[34] Han, Y., Hong, W., Faidley, L., Coupled magnetic field and viscoelasticity of ferrogel, *Int. J. Appl. Mech.* 3, 259-278 (2011).

[35] O. Anwar Bég, S.K. Ghosh and T. A. Bég, *Applied Magneto-Fluid Dynamics: Modelling and Computation,* Lambert Academic Publishing, Saarbrucken, Germany (2011).

[36] G. Fabris and R.G. Hantman, Fluid dynamics aspects of liquid-metal gas two-phase magnetohydrodynamic power generators, *Proc. 1976 Heat Transfer and Fluid Mechanics Institute, University of California, Davis, June 21-23, Stanford University Press, USA* (1976) .

[37] M. Martin, C. Cai, I. Boyd, Slip flow in a magnetohydrodynamic boundary layer, *43rd AIAA Plasmadynamics and Lasers Conference, New Orleans, Louisiana*, USA (2012).

[38] T. Fang, J. Zhang, and S. Yao, Slip MHD viscous flow over a stretching sheet—an exact solution, *Comm. Nonlinear Science and Numerical Simulation*, 14, 3731-3737 (2009).

[39] L.C. Zheng, Y.Q. Liu, and X.X. Zhang, Slip effects on MHD flow of a generalized Oldroyd-B fluid with fractional derivative, *Nonlinear Analysis: Real World Applications,* 13, 513-523 (2012).

[40] R.M. Mckinley, H.O. Jahns, W.W. Harris and R.A. Greenkorn, Non-Newtonian flow in porous media, *AIChemE J.*, 12, 17-20 (1966).

[41] D. Tripathi and O. Anwar Bég, A numerical study of oscillating peristaltic flow of generalized Maxwell viscoelastic fluids through a porous medium, *Transport in Porous Media,* 95, 337-348 (2012).

[42] J. Niu, C. Fu, and W. Tan, Stability of thermal convection of an Oldroyd-B fluid in a porous medium with Newtonian heating, *Physics Letters A*, 374, 4607-4613 (2010).

[43] O. Anwar Bég., Makinde, O. D., Viscoelastic flow and species transfer in a Darcian high permeability channel, *J. Petroleum Science and Engineering*, 76, 93-99 (2011).

[44] W. Kozicki, Viscoelastic flow in packed beds or porous media, *Canadian J Chemical Eng.*, 79, 124–131 (2001).

[45] O. Anwar Bég, H. S. Takhar, R. Bhargava, Rawat, S. and Prasad, V.R., Numerical study of heat transfer of a third grade viscoelastic fluid in non-Darcian porous media with thermophysical effects, *Physica Scripta*, 77, 1-11 (2008).

[46] R. Cao, L. Cheng and P. Lian, Flow behavior of viscoelastic polymer solution in porous

media, *J. Dispersion Science Technology*, 36, 41-50 (2015).

[47] Tong Deng-ke, Shi Li-na. The generalized flow analysis of non-Newtonian visco-elastic fluid flows in porous media, *J. Hydrodynamics*, 19 (6) 695-701 (2004).

[48] S.R.EI Koumy, EI S.I. Barakat, and S.I. Abdelsalam, Hall and porous boundaries effects on peristaltic transport through porous medium of a Maxwell model, *Transp. Porous Media,* 94, 643-658 (2012).

[49] S.B. Khan and M. Khan, Influence of Hall current on rotating flow of a Burger's fluid through a porous space, *J. Porous Media*, 11, 277-287 (2008).

[50] O. Anwar Bég, J. Zueco and S.K. Ghosh Unsteady natural convection of a short-memory viscoelastic fluid in a non-Darcian regime: network simulation, *Chemical Eng. Comm.*, 198, 172-190 (2010).

[51] O. Anwar Bég, Tasveer A. Bég, R. Bhargava, S. Rawat and D. Tripathi, Finite element study of pulsatile magneto-hemodynamic non-Newtonian flow and drug diffusion in a porous medium channel, *J. Mechanics in Medicine and Biology,* 12 (4) 1250081.1 – 1250081.26 (2012).

[52] M.J. Uddin, O. Anwar Bég and A.I. Ismail, Mixed radiative-convective nanofluid flow from a nonlinear stretching or shrinking sheet in porous media with multiple slip boundary conditions, *AIAA J. Thermophysics Heat Transfer* (2015). DOI: 10.2514/1.T4372 (11 pages)

[53]K.C. Cramer and S. Pai, *Applied Magnetofluid Dynamics for Engineers and Applied Physicists*, MacGraw-Hill, New York (1973).

[54] G. Sutton and G. Sherman, *Engineering Magnetohydrodynamics*, MacGraw-Hill, New York (1965).

[55] R.J. Rosa, *Magnetohydrodynamic Energy Conversion*, Hemisphere Publishing, Washington, D.C., USA (1987).

[56] A.C. Eringen, *Microcontinuum Field Theories- II Fluent Media*, Springer, New York (2001).

TABLES

Type of fluid	Rheological parameters	u	v
Newtonian fluid	$\lambda_1 = 0, \lambda_2 = 0, \lambda_3 = 0$	0.348290	-0.0753796
G. Maxwell	$\lambda_1 = 2, \lambda_2 = 0, \lambda_3 = 0$ ($\alpha = \beta = 0.1$)	0.372001	-0.1159010
G. Oldroyd-B	$\lambda_1 = 2, \lambda_2 = 0, \lambda_3 = 1$ ($\alpha = \beta = 0.1$)	0.350487	-0.0773218
Burger	$\lambda_1 = 2, \lambda_2 = 3, \lambda_3 = 1$ ($\alpha = \beta = 1$)	0.343626	-0.0710981
Fractional Burger	$\lambda_1 = 2, \lambda_2 = 3, \lambda_3 = 1$ ($\alpha = \beta = 0.1$)	0.368403	-0.100277

Table 1: Velocity solutions for Case I (general periodic oscillation *with slip condition*) ($Q_0 = -1$, $\omega_0 = 0.1$, $\Omega = 0.3$, $M = t = 0.5$, $z = 0.5$ and $\gamma = 0.5$)

Type of fluid	Rheological parameters	u	v
Newtonian fluid	$\lambda_1 = 0, \lambda_2 = 0, \lambda_3 = 0$	0.327715	-0.0540700
G. Maxwell	$\lambda_1 = 2, \lambda_2 = 0, \lambda_3 = 0$ ($\alpha = \beta = 0.1$)	0.342963	-0.0779771
G. Oldroyd-B	$\lambda_1 = 2, \lambda_2 = 0, \lambda_3 = 1$ ($\alpha = \beta = 0.1$)	0.329034	-0.0551374
Burger	$\lambda_1 = 2, \lambda_2 = 3, \lambda_3 = 1$ ($\alpha = \beta = 1$)	0.325006	-0.0515568
Fractional Burger	$\lambda_1 = 2, \lambda_2 = 3, \lambda_3 = 1$ ($\alpha = \beta = 0.1$)	0.340142	-0.068116

Table 2: Velocity solutions for Case II (Periodic flow between two plates *with slip condition*) ($Q_0 = -1$, $\omega_0 = 0.1$, $\Omega = 0.3$, $M = t = 0.5$, $z = 0.5$ and $\gamma = 0.5$)

Type of fluid	Rheological parameters	u	v
Newtonian fluid	$\lambda_1 = 0, \lambda_2 = 0, \lambda_3 = 0$	0.394565	-0.0930379
G. Maxwell	$\lambda_1 = 2, \lambda_2 = 0, \lambda_3 = 0$ ($\alpha = \beta = 0.1$)	0.548910	-0.1775900
G. Oldroyd-B	$\lambda_1 = 2, \lambda_2 = 0, \lambda_3 = 1$ ($\alpha = \beta = 0.1$)	0.401474	-0.0962267
Burger	$\lambda_1 = 2, \lambda_2 = 3, \lambda_3 = 1$ ($\alpha = \beta = 1$)	0.400604	-0.0660502
Fractional Burger	$\lambda_1 = 2, \lambda_2 = 3, \lambda_3 = 1$ ($\alpha = \beta = 0.1$)	0.443987	-0.1113370

Table 3: Velocity solutions for Case III (Poiseuille flow *with slip condition*) ($Q_0 = -1$, $\omega_0 = 0.1$, $\Omega = 0.3$, $M = t = 0.5$, $z = 0.5$ and $\gamma = 0.5$)

Type of fluid	Rheological parameters	u	v
Newtonian fluid	$\lambda_1 = 0, \lambda_2 = 0, \lambda_3 = 0$	0.39465	-0.0930379
G. Maxwell	$\lambda_1 = 2, \lambda_2 = 0, \lambda_3 = 0$ ($\alpha = \beta = 0.1$)	0.560037	-0.0744996
G. Oldroyd-B	$\lambda_1 = 2, \lambda_2 = 0, \lambda_3 = 1$ ($\alpha = \beta = 0.1$)	0.558487	-0.0742893
Burger	$\lambda_1 = 2, \lambda_2 = 3, \lambda_3 = 1$ ($\alpha = \beta = 1$)	0.563345	-0.0691876
Fractional Burger	$\lambda_1 = 2, \lambda_2 = 3, \lambda_3 = 1$ ($\alpha = \beta = 0.1$)	0.534658	-0.0969811

Table 4: Velocity solutions for Case I (general periodic oscillations with *no slip* condition) ($\omega_0 = 0.1$, $\Omega = 0.3$, $M = t = 0.5$, $z = 0.5$ and $\gamma = 0$)

Type of fluid	Rheological parameters	u	v
Newtonian fluid	$\lambda_1 = 0, \lambda_2 = 0, \lambda_3 = 0$	0.394650	-0.0930379
G. Maxwell	$\lambda_1 = 2, \lambda_2 = 0, \lambda_3 = 0$ ($\alpha = \beta = 0.1$)	0.416045	-0.0514913
G. Oldroyd-B	$\lambda_1 = 2, \lambda_2 = 0, \lambda_3 = 1$ ($\alpha = \beta = 0.1$)	0.428460	-0.3009650
Burger	$\lambda_1 = 2, \lambda_2 = 3, \lambda_3 = 1$ ($\alpha = \beta = 1$)	0.430716	-0.0269874
Fractional Burger	$\lambda_1 = 2, \lambda_2 = 3, \lambda_3 = 1$ ($\alpha = \beta = 0.1$)	0.422294	-0.0416114

Table 5: Velocity solutions for Case II (periodic flow between two plates with *no slip condition*) ($\omega_0 = 0.1$, $\Omega = 0.3$, $M = t = 0.5$, $z = 0.5$ and $\gamma = 0$)

Type of fluid	Rheological parameters	u	V
Newtonian fluid	$\lambda_1 = 0, \lambda_2 = 0, \lambda_3 = 0$	0.394650	-0.0930379
G. Maxwell	$\lambda_1 = 2, \lambda_2 = 0, \lambda_3 = 0$ ($\alpha = \beta = 0.1$)	0.418020	-0.0843680
G. Oldroyd-B	$\lambda_1 = 2, \lambda_2 = 0, \lambda_3 = 1$ ($\alpha = \beta = 0.1$)	0.252292	-0.0338033
Burger	$\lambda_1 = 2, \lambda_2 = 3, \lambda_3 = 1$ ($\alpha = \beta = 1$)	0.239327	-0.0038788
Fractional Burger	$\lambda_1 = 2, \lambda_2 = 3, \lambda_3 = 1$ ($\alpha = \beta = 0.1$)	0.321577	-0.0441474

Table 6: Velocity solutions for Case III (Poiseuille flow with *no slip condition*) ($Q_0 = -1$, $\omega_0 = 0.1$, $\Omega = 0.3$, $M = t = 0.5$, $z = 0.5$ and $\gamma = 0$).

FIGURES
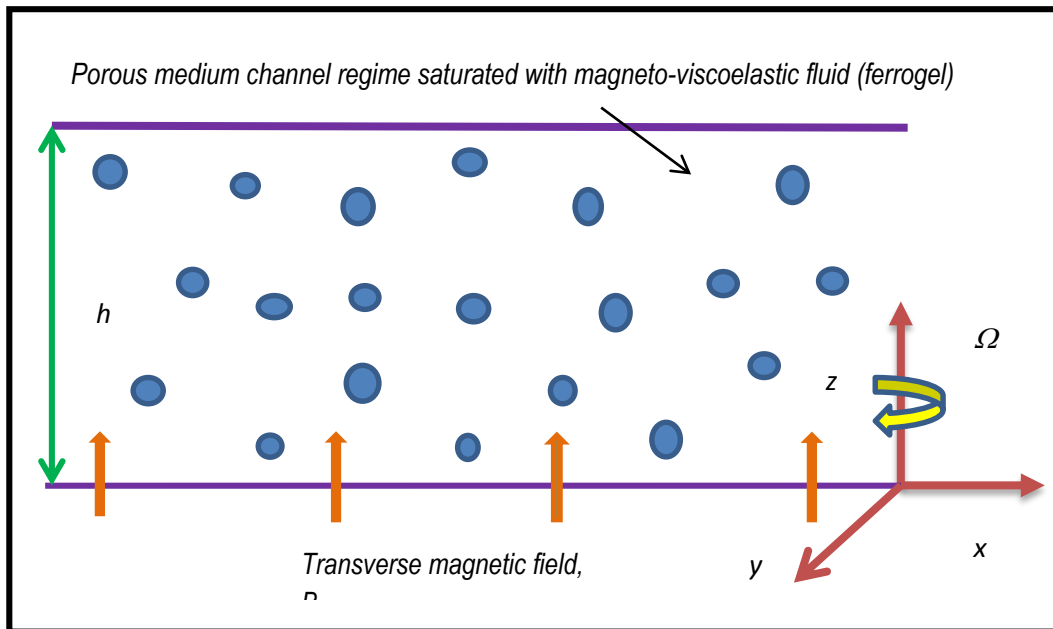
Fig. 1: Physical model for Case II- *periodic rotating magnetohydrodynamic fractional viscoelastic flow in porous media channel between rigid plates.*
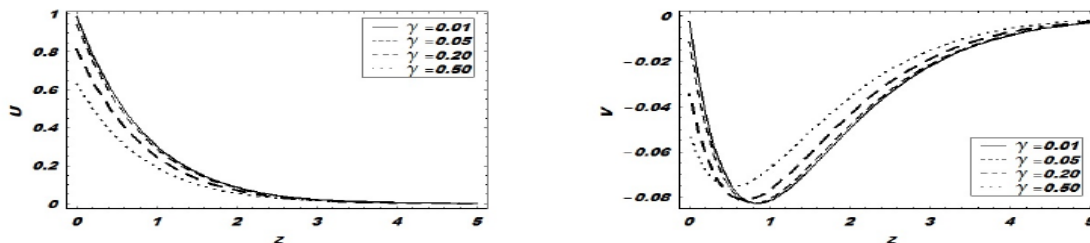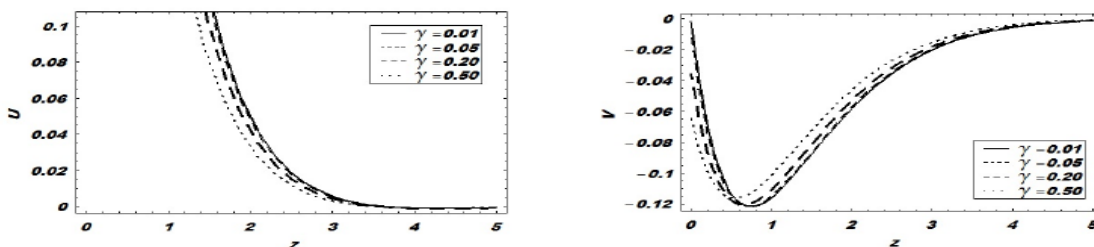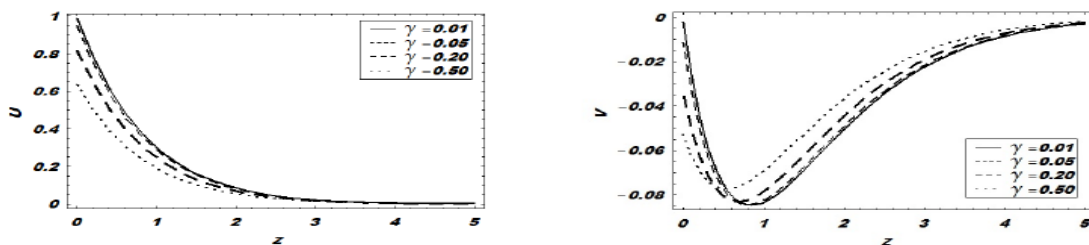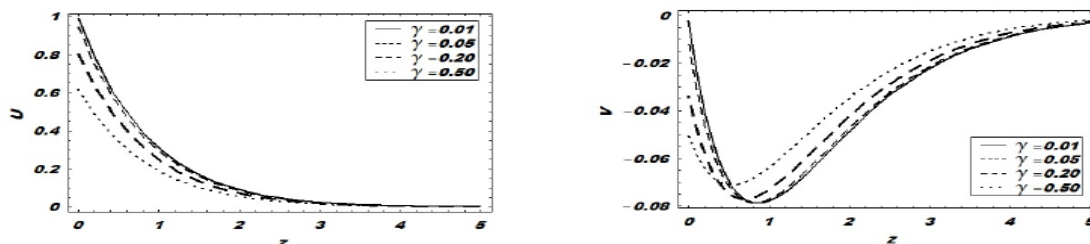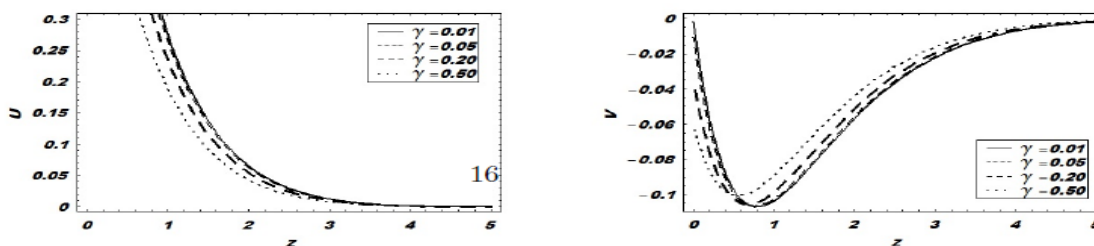
Figs. 2: Influence of slip parameter (γ) on velocity evolution for *Case I* (general periodic oscillations from a rigid plate) with $M = t = 0.5$, $\omega_o = 0.1$ and $\Omega = 0.3$.
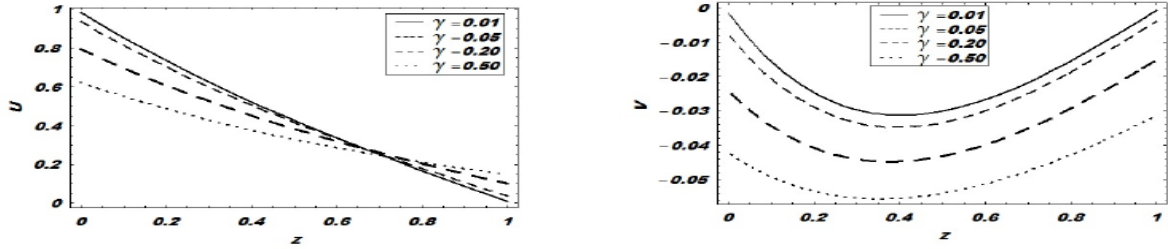
Newtonian fluid$(\lambda_1 = 0, \lambda_2 = 0, \theta = 0)$
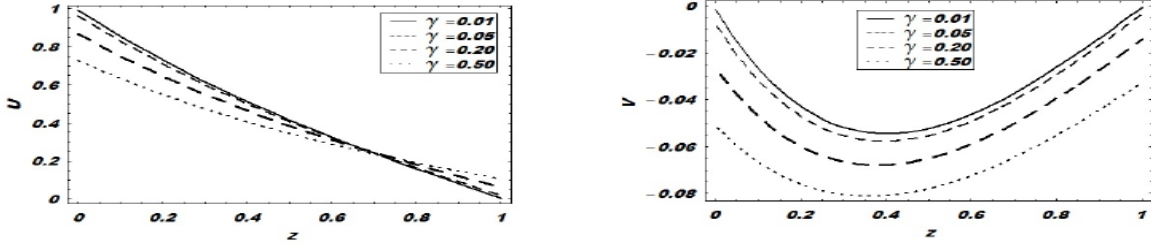
G. Maxwell fluid$(\alpha = \beta = 0.1, \lambda_1 = 2, \lambda_2 = 0, \lambda_3 = 0)$
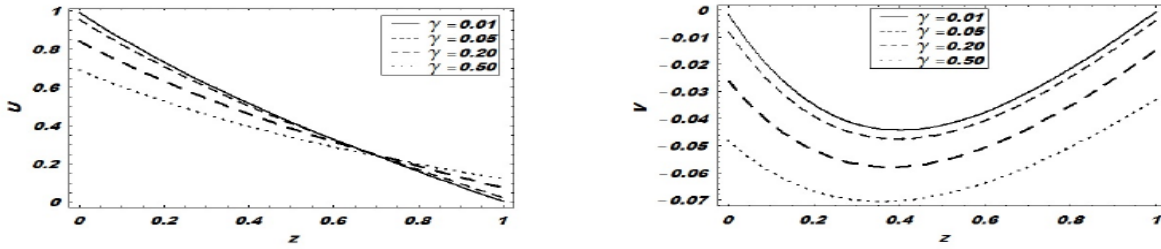
G. Oldroyd-B fluid$(\alpha = \beta = 0.1, \lambda_1 = 2, \lambda_2 = 0, \lambda_3 = 1)$
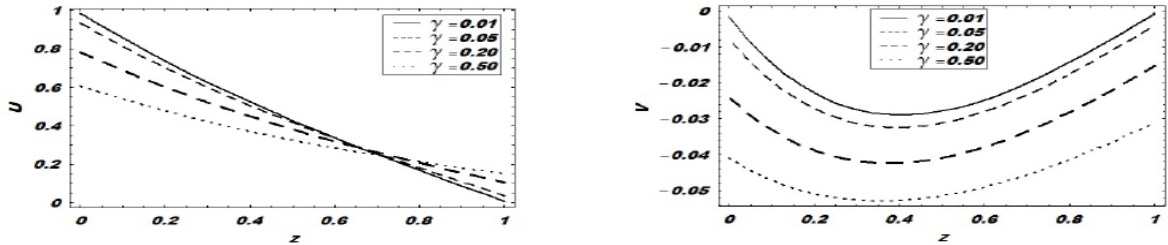
Burger's fluid$(\alpha = \beta = 1, \lambda_1 = 2, \lambda_2 = 3, \lambda_3 = 1)$
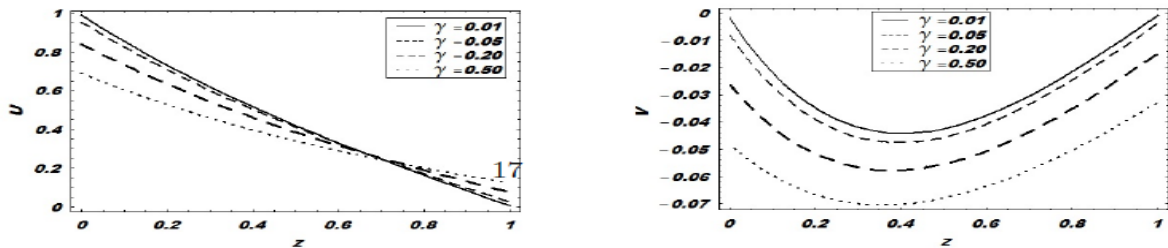
Fractional burger's fluid$(\alpha = \beta = 0.1, \lambda_1 = 2, \lambda_2 = 3, \lambda_3 = 1)$

Figs. 3: Influence of slip parameter (γ) on velocity evolution for *Case II* (periodic channel flow) with $M = t = 0.5$, $\omega_0 = 0.1$ and $\Omega = 0.3$.

Newtonian fluid$(\lambda_1 = 2, \lambda_2 = 3, \theta = 0)$

G. Maxwell fluid$(\alpha = \beta = 0.1, \lambda_1 = 2, \lambda_2 = 0, \lambda_3 = 0)$

G. Oldroyd-B fluid$(\alpha = \beta = 0.1, \lambda_1 = 2, \lambda_2 = 0, \lambda_3 = 1)$

Burger's fluid$(\alpha = \beta = 1, \lambda_1 = 2, \lambda_2 = 3, \lambda_3 = 1)$

Fractional burger's fluid$(\alpha = \beta = 0.1, \lambda_1 = 2, \lambda_2 = 3, \lambda_3 = 1)$
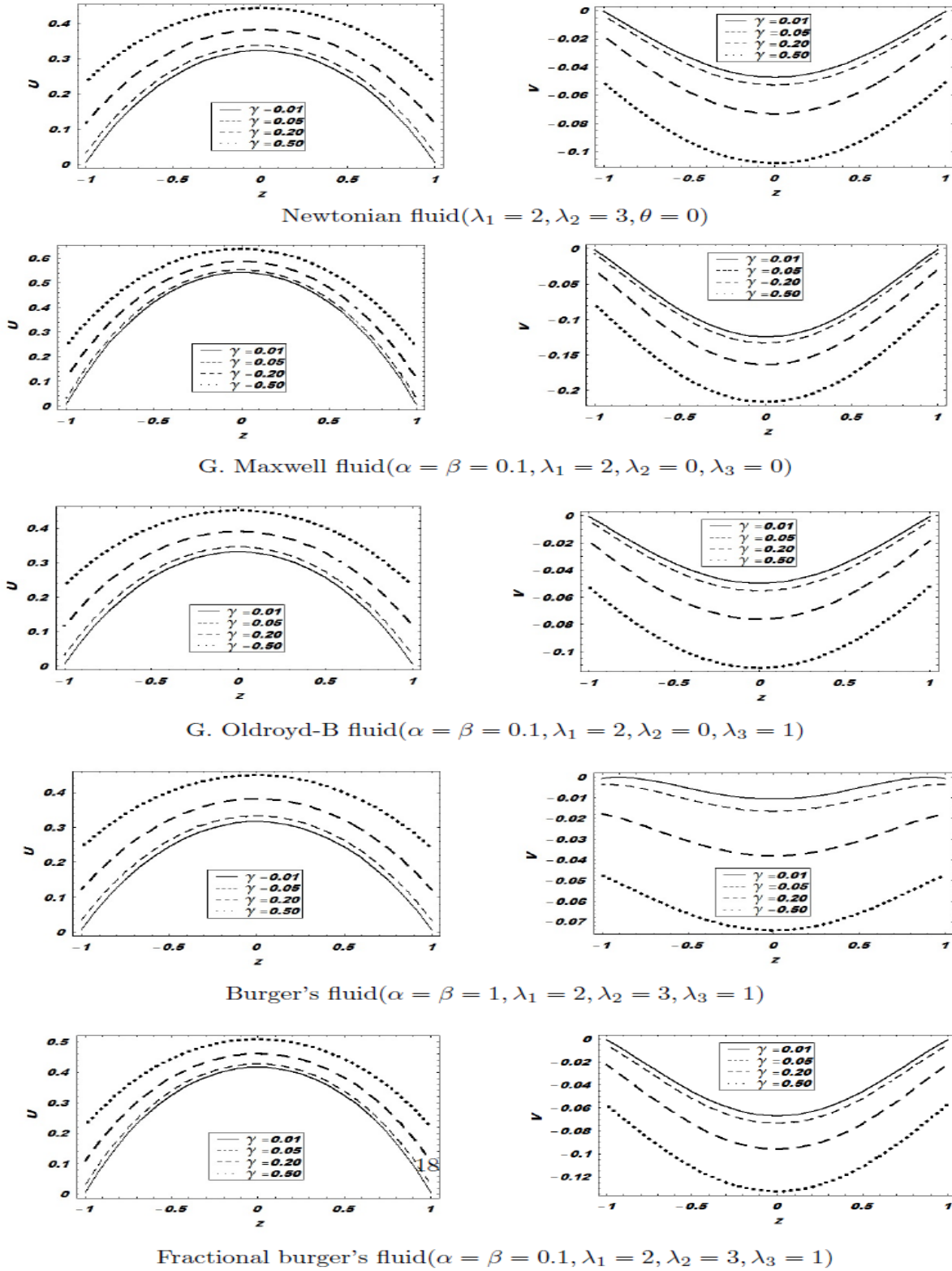
Figs. 4: Influence of slip parameter (γ) on velocity evolution for *Case III* (Poiseuille channel flow) with $Q_0 = -1$, $M = t = 0.5$, $\omega_0 = 0.1$ and $\Omega = 0.3$.